

N₂O₅ Reactive Uptake on Aqueous Sulfuric Acid Solutions Coated with Branched and Straight-Chain Insoluble Organic Surfactants

L. M. Cosman, D. A. Knopf,[†] and A. K. Bertram*

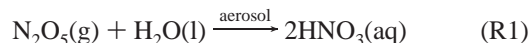
Department of Chemistry, University of British Columbia, 2036 Main Mall,
Vancouver, British Columbia V6T 1Z1, Canada

Received: November 8, 2007; In Final Form: December 19, 2007

A flow reactor coupled to a chemical ionization mass spectrometer was used to study the reactive uptake coefficients at 273 K of N₂O₅ on aqueous 60 wt % sulfuric acid solutions coated with insoluble organic monolayers. Both straight-chain surfactants (1-hexadecanol, 1-octadecanol, and stearic acid) and a branched surfactant (phytanic acid) were studied. The reactive uptake coefficient decreased dramatically for straight-chain surfactants. The decrease ranged from a factor of 17 to a factor of 61 depending on the type of straight-chain surfactant. In contrast to the straight-chain data, the presence of phytanic acid did not have a significant effect on the N₂O₅ reactive uptake coefficient (the decrease was less than the uncertainty in the data) compared to the uncoated solution. In addition to measuring the reactive uptake coefficients, we also investigated the relationship between properties of the monolayers and the reactive uptake coefficients. The reactive uptake coefficients measured on aqueous sulfuric acid subphases showed a relationship to the surface area occupied by the surfactant molecules. However, data obtained with other subphases did not overlap with this trend.

1. Introduction

Reactions between aerosol particles and gas-phase species, termed heterogeneous reactions, can play a crucial role in the atmosphere.^{1–4} Often, the efficiency of these heterogeneous reactions is described in terms of the reactive uptake coefficient, γ , which is defined as the fraction of collisions with a surface that lead to the irreversible loss of the gas-phase species as the result of a reaction. One heterogeneous reaction that has been studied extensively is the reaction between N₂O₅ and aqueous particles



Modeling studies have demonstrated that this reaction can affect NO_x, O₃, and OH concentrations in the atmosphere.^{5–7} For example, using a global tropospheric model, Dentener and Crutzen⁵ demonstrated that this heterogeneous reaction would decrease the yearly average NO_x, O₃, and OH concentrations in the troposphere by 49%, 9%, and 9%, respectively, if the reactive uptake coefficient on aqueous particles were 0.1.

Because of the importance of this heterogeneous reaction to the atmosphere, many research groups have investigated the reactive uptake coefficient of N₂O₅ on aqueous inorganic solutions and particles (see Sander et al.⁸ and references therein). These studies have shown that N₂O₅ reactive uptake is efficient on aqueous inorganic solutions, with reactive uptake coefficients ranging from 0.015 to 0.2.⁸

Most of the previous laboratory work on N₂O₅ reactive uptake has focused on aqueous inorganic solutions and particles free

of organic surfactants. Nevertheless, field studies indicate that tropospheric inorganic aerosols can contain a significant amount of organic surfactants—both insoluble aqueous surfactants and/or soluble aqueous surfactants. (See, for example, refs 9–23.) These surfactants can form organic monolayers at the air–aqueous interface,^{21–23} and depending on the composition and degree of compression of these organic monolayers, they can limit the transfer of molecules across the air–aqueous interface.^{21–36} If this were the case, the N₂O₅ reactive uptake coefficients measured on uncoated aqueous inorganic solutions might not be applicable under all atmospheric conditions. Examples of atmospheric conditions under which surfactants might be important include the marine boundary layer and continental regions influenced by forest fires, coal and straw burning.^{9,13,16,18–20}



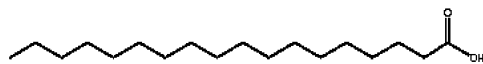
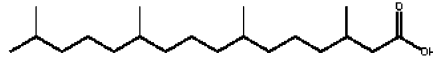
Recent possibly related field measurements over the northeast United States by Brown et al.³⁷ showed that the reactive uptake coefficient of N₂O₅ can decrease significantly (by a factor of ≥ 10) when particles contain a large amount of organic material in addition to inorganic material. One possible explanation for these results is that the organic material forms a coating on the aqueous droplets and this coating limits the transfer of N₂O₅ molecules across the air–aqueous interface.³⁷ More laboratory studies on the effects of organic films on N₂O₅ heterogeneous chemistry would be useful to better understand the precise mechanism that led to the decrease in γ observed by Brown et al.³⁷

A few laboratory studies have examined the reactive uptake of N₂O₅ on aqueous surfaces coated with monolayers consisting of straight-chain organic surfactants.^{24,30–32} However, only one study has investigated the effect of monolayers consisting of a bent or branched surfactant on the N₂O₅ uptake coefficient,³⁸ even though a large fraction of atmospheric surfactants might have bent or branched structures.^{22,39} Furthermore, all of the previous measurements, except for the preliminary study carried

* To whom correspondence should be addressed. E-mail: bertram@chem.ubc.ca.

[†] Present address: Institute for Terrestrial and Planetary Atmospheres, School of Marine and Atmospheric Sciences, Stony Brook University, Stony Brook, NY 11794.

TABLE 1: Structures of the Organic Molecules Used in This Study

Organic compound	Melting points ^a (°C)	Molecular Structure
1-hexadecanol	48-50	
1-octadecanol	56-59	
stearic acid (octadecanoic acid)	67-72	
phytanic acid (3,7,11,15-tetramethylhexadecanoic acid)	< 20	

^a Melting points for 1-hexadecanol, 1-octadecanol, and stearic acid were obtained from Sigma-Aldrich; no melting point has been reported for phytanic acid, but it is a liquid at room temperature.

out in our laboratory³² focused on soluble organic surfactants. Additional studies with insoluble organic surfactants would be beneficial.

In addition to the monolayer studies mentioned above, Folkers et al.²⁷ investigated the reactive uptake of N₂O₅ on aqueous inorganic aerosols coated with multilayers of organic material produced by the ozonolysis of α -pinene. Also, Badger et al.⁴⁰ studied the reactive uptake of N₂O₅ on aerosol particles containing mixtures of humic acid (a water-soluble surfactant) and ammonium sulfate.

The current article focuses on the uptake of N₂O₅ on aqueous solutions coated with insoluble organic monolayers. Specifically, we focus on the reactive uptake coefficient at 273 K of N₂O₅ on aqueous 60 wt % sulfuric acid solutions coated with monolayers of 1-hexadecanol, 1-octadecanol, stearic acid, and phytanic acid (see Table 1 for chemical structures). 1-Hexadecanol, 1-octadecanol, and stearic acid are all straight-chain insoluble organic surfactants, whereas phytanic acid is a branched insoluble surfactant. The temperature of 273 K is relevant for the lower and middle troposphere. This temperature was chosen because of both its atmospheric relevance and experimental constraints. At warmer temperatures, the vapor pressure of water over aqueous solutions is large, which significantly limits the range of reactive uptake coefficients that can be measured with our experimental apparatus because of large gas-phase diffusion corrections (see below for further details).

For these studies, we used a rectangular channel flow reactor to measure reactive uptake coefficients. One of the strengths of the experimental configuration is that we can prepare and study well-characterized organic monolayers with this apparatus. In this work, we present measurements of the surface pressures of the prepared monolayers and the surface areas occupied by each surfactant molecule in the monolayers (i.e., the packing densities of the monolayers). Then, we present measurements of the reactive uptake coefficients. We then try to correlate trends in the measured reactive uptake coefficients with surfactant chain length, surface pressure of the monolayer, and surface area occupied by each surfactant molecule to better understand the variables governing the reactive uptake coefficient. The atmospheric implications of these results are also discussed.

2. Experimental Section

Flow Reactor and Experimental Conditions for the Reactive Uptake Measurements. Figure 1 presents a schematic of the flow reactor. Figure 1a shows a top view with the cover

removed, and Figure 1b shows a side view. The apparatus was described and characterized in detail in our previous publication.³² The flow cell is made entirely from aluminum, and its temperature can be controlled by circulating coolant through channels in the aluminum body. All interior aluminum walls are coated with halocarbon wax to minimize loss of N₂O₅ to the walls. Located on the bottom surface of the reactor is a glass trough that is filled with the aqueous solution, and this aqueous solution can be covered with an organic monolayer. The surface of the liquid in the trough is 7.5 cm in width and 22 cm in length. The height of the head space (or open channel) above the liquid surface (Figure 1b) depends on the amount of liquid solution used in each experiment and, in most cases, is less than 1 cm. N₂O₅ is introduced to the flow reactor by a movable T-shaped injector, which slides just above the liquid surface. The T-shaped injector is equipped with six exit holes, each 0.2 mm in diameter, that point toward the top of the reactor and distribute the gas-phase reactant evenly across the width of the flow cell. The carrier gas (He) enters the flow reactor through inlets at the back of the flow cell. This gas stream within the reactor first flows against a barrier to ensure mixing before reaching the liquid surface. Thermocouples are used to determine the temperatures of the liquid and the gas above the liquid. In all cases, temperatures of the liquid and gas are within ± 0.5 K of each other. The pressure inside the flow cell is measured using an MKS baratron at the exit of the flow reactor (see Figure 1b).

Prior to entering the flow cell, the carrier gas was first passed through a carbon filter (Supelco, Supelcarb HC) and a Drierite (W.A. Hammond Drierite Co. Ltd.) trap cooled with liquid nitrogen to remove any possible organic contamination. Then, the carrier gas was passed over a water reservoir held at a fixed temperature to adjust the relative humidity (RH) of the carrier gas. The RH was adjusted so that it matched the relative humidity over the specific aqueous sulfuric acid solution, calculated using the AIM model.^{41–43} This ensured that no evaporation of water from the aqueous sulfuric acid solution occurred over the course of the experiments. For these experiments, the relative humidity above the aqueous solution was maintained at $(14.5 \pm 1.5)\%$. The RH of the carrier gas was verified with a dew-point hygrometer.

The open channel above the liquid surface has a rectangle geometry. The flow dynamics of the gas above the liquid surface was characterized in our previous publication using computation fluid dynamics simulations.³² These calculations showed that the carrier gas reaches a fully developed laminar flow in less

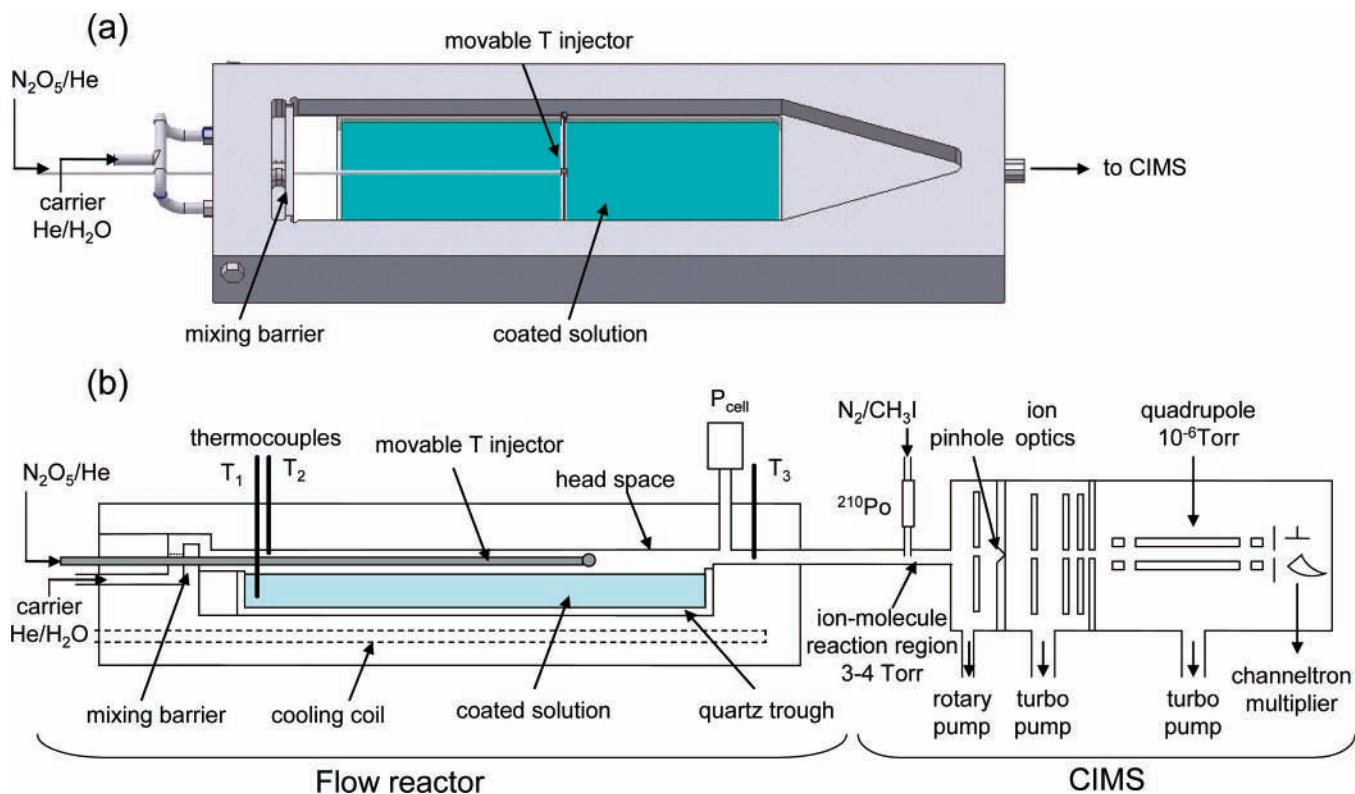


Figure 1. (a) Top view of the rectangular channel flow reactor without the aluminum cover. The liquid solution is placed in a quartz trough located inside the flow reactor. (b) Side view of the rectangular channel flow reactor coupled to the chemical ionization mass spectrometer (CIMS).

than 1.5 cm, which is much shorter than the length of the reactive surface (i.e., liquid surface). See our previous publication for further discussion on the gas flow dynamics in the system.³²

N_2O_5 was produced by reacting NO_2 with an excess of O_3 . O_3 was generated by passing a flow of O_2 over an ultraviolet source (Jelight, model #600). To remove water vapor from the O_2 carrier gas, a Drierite trap was placed immediately before the UV lamp. The NO_2 flow was passed through a P_2O_5 trap to remove trace amounts of water prior to reaction with O_3 . N_2O_5 produced by this reaction was flowed through an additional P_2O_5 trap to reduce the concentration of nitric acid and was then collected and stored in a glass trap immersed in an ethanol bath cooled to 193 K. N_2O_5 condensed as white crystals inside the glass trap.

During uptake experiments, a saturated flow of N_2O_5 between 6 and 10 $\text{cm}^3 \text{min}^{-1}$ at STP was mixed with 20–100 $\text{cm}^3 \text{min}^{-1}$ at STP of dry He prior to entering the flow reactor through the T-shaped injector. Total mass flow rates inside the flow reactor ranged from 200 to 700 $\text{cm}^3 \text{min}^{-1}$ at STP, and total pressures ranged from 2.4 to 3.1 Torr. Under these conditions, the Reynolds number varied from 0.4 to 1.4, indicating laminar flow conditions.

The exit of the flow cell is connected to a chemical ionization mass spectrometer (CIMS), which is used to measure the change in the gas-phase reactant concentration as a result of reactive uptake at the liquid surface.^{44,45} N_2O_5 was detected as NO_3^- after its chemical ionization by I^- .^{46–48} I^- was formed by flowing trace amounts of CH_3I diluted in 1000–2000 $\text{cm}^3 \text{min}^{-1}$ at STP of N_2 through a polonium-210 source (NRD, model Po-2031) for ionization. For N_2O_5 detection in the presence of H_2O , the chemical ionization region was biased to -122 V in order to fragment weakly bound ion– H_2O clusters.^{47,48} N_2O_5 concentrations of (2×10^{10}) – (1×10^{11}) molecules cm^{-3} were used for the uptake measurements. N_2O_5 concentrations were based

on the $\text{I}^- + \text{N}_2\text{O}_5$ chemical ionization reaction rate that has been reported in the literature.⁴⁶

In a typical uptake experiment, we measured the N_2O_5 signal as a function of injector position. The natural logarithm of this signal was then plotted as a function of reaction time (time was calculated from the reaction length and the flow velocity), in order to determine the observed first-order loss rate constant, k_{obs} . Then, from k_{obs} , we determined the first-order wall loss rate constant, k_w , using the procedure developed in our previous work.³² This procedure corrects for any concentration gradients that can develop in the flow reactor as a result of fast heterogeneous loss at the liquid surface. In other words, this procedure decouples reaction and diffusion to the aqueous surface in order to determine the true first-order wall loss rate constant.

To calculate k_w from k_{obs} , diffusion coefficients were needed. The diffusion coefficients applied in this study were taken from Knopf et al.³² and are based on calculations using molecular parameters.^{49–51} For the diffusion coefficient of N_2O_5 in He ($D_{\text{N}_2\text{O}_5\text{-He}}$) at 273 K, we used a value of 289 Torr $\text{cm}^2 \text{s}^{-1}$, and for the diffusion coefficient of N_2O_5 in H_2O ($D_{\text{N}_2\text{O}_5\text{-H}_2\text{O}}$) at 273 K, we used a value of 72 Torr $\text{cm}^2 \text{s}^{-1}$. To calculate the diffusion coefficient, D , of N_2O_5 in a mixture of helium and water, we used the equation⁵²

$$\frac{1}{D} = \frac{P_{\text{He}}}{D_{\text{N}_2\text{O}_5\text{-He}}} + \frac{P_{\text{H}_2\text{O}}}{D_{\text{N}_2\text{O}_5\text{-H}_2\text{O}}} \quad (1)$$

where P_{He} and $P_{\text{H}_2\text{O}}$ are the partial pressures of helium and water vapor, respectively, in the flow reactor.

The reactive uptake coefficient, γ , was determined from k_w using the equation^{53,54}

$$\frac{1}{\gamma} = \frac{c}{4k_w} \cdot \frac{S}{V} + \frac{1}{2} \quad (2)$$

where c is the mean molecular velocity of N₂O₅, S is the reactive surface area inside the flow reactor, and V is the volume of the open channel above the liquid surface (i.e., the volume of the head space illustrated in Figure 1b).

Preparation of the Organic Monolayers. Prior to preparation of an organic monolayer, the surface of the aqueous solution (60 wt % sulfuric acid) was thoroughly cleaned with an aspirator to remove any organic contamination on the surface. Solutions of 1-octadecanol, 1-hexadecanol, stearic acid, and phytanic acid dissolved in chloroform (~1 mg cm⁻³) were prepared. Several droplets of the organic solution were deposited on the clean aqueous sulfuric acid surface. The chloroform evaporated, leaving behind an organic monolayer. An excess amount of organic material was used so that a few microcrystals or lenses in the case of a solid or liquid organic monolayer, respectively, were left on the surface after a monolayer was established. Typically 25% more organic material was added than required to attain a tightly packed monolayer. The presence of microcrystals or lenses on the surface (which was verified visually) ensured that the aqueous solutions were completely coated with a surfactant monolayer. This method was chosen because of the reproducibility and ease of preparing this type monolayer. Monolayers in contact with microcrystals or lenses were used in all reported reactive uptake coefficient measurements. The presence of these crystals or lenses was not expected to affect the overall uptake coefficient of N₂O₅ as the surface area covered by the crystals or lenses was very small compared to the overall surface area exposed to N₂O₅. To confirm this point, we carried out experiments in which we varied the amount of excess organic material used in the uptake experiments. For example, we carried out some experiments in which only enough organic material was added to the aqueous surface to form a tightly packed monolayer (i.e., no microcrystals or lenses were formed). In these experiments, the reactive uptake coefficients were within the experimental uncertainties of the uptake coefficients determined in the presence of the microcrystals or lenses. This confirms that the presence of the microcrystals or lenses had little effect on our uptake measurements. Also, if small islands consisting of multilayers of surfactant did form in our experiments when excess organic was used, they did not influence our results.

Measurements of the Surface Pressure of the Monolayers and the Surface Area Occupied by Each Surfactant Molecule in the Films. Prior to measuring the reactive uptake coefficients, we first determined the surface pressure of the prepared monolayers (monolayers in contact with microcrystals or lenses) and the surface area occupied by each surfactant molecule in these monolayers, in order to better understand the physical properties of the monolayers under investigation.

The surface pressure (π) of an organic monolayer at 273 K in the rectangular flow reactor was determined by first measuring the surface tension of the solution coated by an organic film (σ_{film}) and the surface tension of the uncoated film (σ_o). Surface pressure was then calculated using the equation⁵⁵

$$\pi = \sigma_o - \sigma_{\text{film}} \quad (3)$$

The surface tensions of the coated and uncoated films were determined by the Wilhelmy plate method. In short, we measured the force (using a surface pressure sensor; NIMA Technology, model PS4) on a platinum plate as the plate was immersed into and detached from the liquid solution. The surface

tension was calculated from the maximum difference in the force on the plate between immersion into and separation from the solution.^{56,57} For the solutions coated with the organic monolayers, we measured the surface tension just before and after the reactive uptake experiments. In all cases, the results were the same within experimental error. The following procedure was employed to measure surface tensions within the rectangular channel flow reactor: First, we degassed the aqueous solution. Second, we prepared the monolayers; assembled the flow cell; and established experimental conditions such as RH, temperature, and mass flow in order to condition the flow cell. Then, after about 1 h of conditioning, we removed the cover of the flow cell, measured the surface tension of the coated film, reassembled the flow cell, and performed the uptake experiments.

To determine the surface area occupied by each surfactant molecule in the monolayers, we measured, in a separate set of experiments, the surface pressure–area isotherm for each organic surfactant on an aqueous 60 wt % H₂SO₄ solution at 273 K. The pressure–area isotherm illustrates the variation of the surface pressure with the area occupied by each surfactant molecule. Pressure–area isotherms were carried out using a commercial temperature-controlled Langmuir film balance (NIMA Technology, model 611D). The Langmuir film balance consisted of a PTFE trough (with dimensions of 20 cm by 30 cm), two movable barriers, and a surface pressure sensor (NIMA Technology, model PS4) with a platinum plate. The experimental procedure that was followed was described in detail by Myrick and Franses.⁵⁸ Briefly, the aqueous sulfuric acid solution was placed in the trough. The surface of the acid solution was cleaned thoroughly using an aspirator. A known volume of an organic solution (containing the surfactant and chloroform) was added to the clean H₂SO₄–H₂O surface. The chloroform was allowed to evaporate, leaving behind a known number of molecules on the surface. The surface pressure was then recorded as the moveable barriers reduced the available surface area, resulting in a surface pressure–area isotherm.⁵⁵ Examples of typical pressure–area isotherms determined in our studies are presented in Figure 2. Once the pressure–area isotherms and the surface pressure of the prepared films were known, the corresponding molecular surface area occupied by each surfactant molecule within the monolayer can be easily read from the surface pressure–area isotherms.

Further Characterization of the Organic Monolayers in the Flow Reactor. During the reactive uptake coefficient measurements, there was a steady gas flow above the organic monolayers. A flow above a monolayer could produce an additional horizontal force on the monolayers (i.e., surface stress), which could cause a film pressure gradient along the length of the flow reactor.⁵⁹ However, because we used low flow rates and low pressures, this force was minor and, at most, could cause the surface pressure of the film to increase by approximately 0.03 mN/m,⁵⁹ which is small compared to the surface pressures used in our experiments. Also note that, in our experiments, we used a range of flow velocities. For example, for a phytanic acid monolayer, we used flow velocities ranging from 165 to 425 cm s⁻¹. We did not see any dependence of the reactive uptake coefficient on the flow velocity. If the force from the steady gas flow on the monolayer were significant in our experiments, we would expect to see a dependence of the uptake coefficient on the flow velocity because the surface stress is proportional to the square of the velocity.

Chemicals. Listed below are the chemicals, manufacturers, and corresponding purities of the chemicals used in our

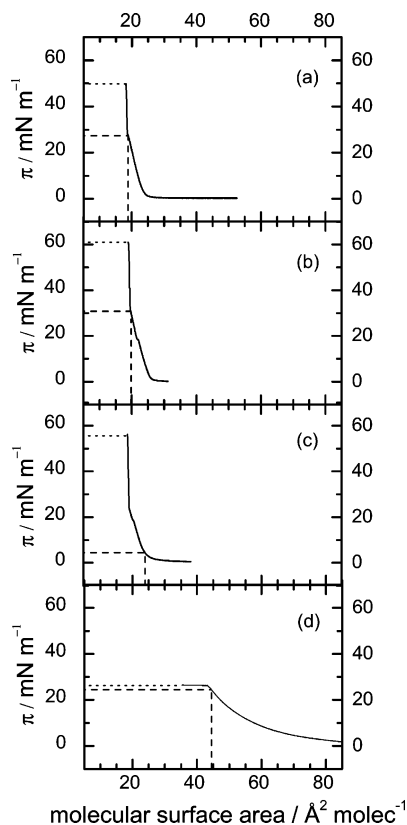


Figure 2. Surface pressure–area isotherms for (a) 1-hexadecanol, (b) 1-octadecanol, (c) stearic acid, and (d) phytanic acid measured on aqueous 60 wt % sulfuric acid at 273 K. The horizontal dashed lines represent the surface pressures of the monolayers measured in the kinetic uptake experiments, and the vertical dashed lines represent the corresponding molecular surface areas at those surface pressures. The collapse pressures are indicated by the horizontal dotted lines.

studies: Helium (Praxair, 99.99% purity), nitrogen (Praxair, 99.999%), nitrogen dioxide (Matheson, 99.5%), oxygen (Praxair, 99.5%), diphosphorus pentoxide (Aldrich, 97%), 1-hexadecanol (Sigma-Aldrich, >99%), 1-octadecanol (Sigma-Aldrich, 99%), stearic acid (Sigma-Aldrich, >98%), phytanic acid (Sigma-Aldrich, 96%), chloroform (Fischer, >99%), and sulfuric acid (Fischer, >95%).

3. Results and Discussion

Properties of the Monolayers. In Table 2 are listed the surface pressures of the prepared monolayers (monolayers in contact with a few microcrystals or liquid lenses) on aqueous 60 wt % H_2SO_4 at 273 K measured in our experiments. The surface pressures for 1-hexadecanol, 1-octadecanol, stearic acid, and phytanic acid on 60 wt % sulfuric acid–water solutions at 273 K are 27.4 ± 0.6 , 30.8 ± 1.6 , 4.4 ± 0.5 , and 23.9 ± 0.7 mN m^{-1} , respectively. The stearic acid monolayer has a much lower surface pressure than those of the other surfactants.

Shown in Figure 2 are surface pressure–area (π – A) isotherms for 1-hexadecanol, 1-octadecanol, stearic acid, and phytanic acid on aqueous 60 wt % sulfuric acid solutions at 273 K. π – A isotherms were also obtained for 1-octadecanol on water at 295 K (not shown) and compared with literature data for validation of our experimental procedure. The results for 1-octadecanol on water agree well with those in the literature.⁶⁰ Also, the isotherms for 1-hexadecanol, 1-octadecanol, stearic acid, and phytanic acid on aqueous 60 wt % show trends (i.e., the positions of the “kinks” in the π – A isotherm; see description

below) similar to those of the isotherms for the same compounds on water and other aqueous solutions reported in the literature.^{55,60,61}

For the straight-chain surfactants, at a high value for the molecular surface area per molecule, the surface pressure is nearly zero. For a molecular surface area close to approximately $25 \text{ \AA}^2 \text{ molecule}^{-1}$, the surface pressure increases rapidly until the monolayer collapses. The collapse pressure is indicated by the horizontal dotted lines in Figure 2. The collapse pressure of a monolayer depends not only on the nature of the surfactant molecules and the temperature and composition of the subphase, but also on experimental conditions such as the rate of compression, the previous history of the film, and the presence of impurities on the surface.⁵⁵ In our experiments, we observed the collapse pressure to vary between 36 and 60 mN m^{-1} for the straight-chain monolayers and between 25.7 and 26.5 mN m^{-1} for the branched monolayer. Aside from the collapse pressures, the isotherms did not change significantly when the rate of compression was varied from 20 to 50 $\text{cm}^2 \text{ min}^{-1}$. In π – A isotherms for the straight-chain surfactants, there are several “kinks” in the isotherms, due to 2-D phase transitions.^{55,61} These phase transitions correspond to different degrees of ordering of the organic molecules.^{60,61} At large molecular surface areas, the films exist as a 2-D gas on the aqueous acid surface, with molecules on the surface exerting relatively little force on each other because they are separated sufficiently.⁵⁵ For decreasing molecular surface areas, the monolayers undergo several phase transitions until they reach their collapse pressure. The phases associated with these phase transitions are generally referred to as gaseous, expanded liquid, condensed liquid, and condensed solid phases.⁵⁵

The behavior for the branched-chain monolayer is significantly different from that for the straight-chain surfactants. Between 45 and 80 $\text{\AA}^2 \text{ molecule}^{-1}$, the branched-chain monolayer is in a liquid expanded state.⁵⁵ At a surface pressure of $\sim 26 \text{ mN m}^{-1}$, the monolayer collapses, and further compression of the film results in the formation of liquid lenses in equilibrium with a monolayer at a molecular surface area of $\sim 44.5 \text{ \AA}^2 \text{ molecule}^{-1}$. The π – A area isotherm obtained here is in good agreement with the π – A area isotherms of other branched surfactants reported in the literature.⁵⁵ Branched surfactants typically do not form condensed solid or condensed liquid states, because the side chains hinder a close-packed molecular arrangement of the surfactant molecules.⁵⁵

Also indicated in Figure 2 as horizontal dashed lines are the measured surface pressures of the monolayers prepared for the reactive uptake experiments (i.e., films in contact with microcrystals or liquid lenses). The corresponding molecular surface areas occupied by the organic surfactants in these monolayers are given by vertical dashed lines and thus can be readily read off the figure. The molecular surface area occupied by each surfactant molecule is also included in Table 2. 1-hexadecanol and 1-octadecanol are the most tightly packed films, with molecular surface areas per molecule of 18.8 ± 0.5 and $19.7 \pm 0.5 \text{ \AA}^2 \text{ molecule}^{-1}$, respectively. Stearic acid is intermediate, with a surface area of $24.1 \pm 0.5 \text{ \AA}^2 \text{ molecule}^{-1}$. Phytanic acid has a much larger surface area per molecule, $44.8 \pm 0.5 \text{ \AA}^2 \text{ molecule}^{-1}$, compared to the straight-chain monolayers, indicating that the phytanic acid is less densely packed on the aqueous acidic surface. Phytanic acid is less efficient at packing because of the branched nature of the molecule, as mentioned above. The four methyl side chains on the long hydrocarbon tail of phytanic acid prevent it from attaining a tightly packed molecular arrangement. The effects of the chain length, surface

TABLE 2: Surface Pressure of Each Organic Monolayer and Surface Area Occupied by Each Surfactant Molecule during Reactive Uptake of N₂O₅ on 60 wt % Sulfuric Acid Solutions at 273 K in the Presence and Absence of Organic Monolayers

monolayer	π of monolayer (mN m ⁻¹)	surface area of monolayer (Å ² /molecule)	γ	lower limit	upper limit	$\gamma_{\text{film}}/\gamma_{\text{uncoated}}$
none ^a	—	—	4.9×10^{-2}	3.8×10^{-2}	10.4×10^{-2}	1
1-hexadecanol	27.4 ± 0.6	18.8 ± 0.5	8.9×10^{-4}	8.0×10^{-4}	9.8×10^{-4}	0.018
1-octadecanol	30.8 ± 1.6	19.8 ± 0.5	8.0×10^{-4}	6.3×10^{-4}	9.7×10^{-4}	0.016
stearic acid	4.4 ± 0.5	24.1 ± 0.5	3.0×10^{-3}	2.1×10^{-3}	3.8×10^{-3}	0.060
phytanic acid	23.9 ± 0.7	44.8 ± 0.5	5.4×10^{-2}	3.9×10^{-2}	1.5×10^{-2}	1.100

^a Knopf et al.³²**TABLE 3: Comparison of Measured Reactive Uptake Coefficients of N₂O₅ on Aqueous H₂SO₄ and NaCl Solutions Coated with Straight-Chain Organic Monolayers of Different Chain Lengths**

ref	monolayer	subphase	T (K)	chain length	$\gamma_{\text{film}}/\gamma_{\text{uncoated}}$
this study	1-octadecanol	H ₂ SO ₄ /H ₂ O	273	18	0.016
this study	stearic acid	H ₂ SO ₄ /H ₂ O	273	18	0.060
Knopf et al. ³²	1-octadecanol	H ₂ SO ₄ /H ₂ O	298	18	0.018
this study	1-hexadecanol	H ₂ SO ₄ /H ₂ O	273	16	0.018
McNeill et al. ²⁴	SDS	NaCl/H ₂ O	295	12	0.133
Thornton and Abbott ³⁰	hexanoic acid	NaCl/H ₂ O	300	6	0.333
Park et al. ³¹	hexanol	H ₂ SO ₄ /H ₂ O	216	6	0.400
Park et al. ³¹	butanol	H ₂ SO ₄ /H ₂ O	216	4	0.667

pressure, and molecular surface area on the reactive uptake coefficients are explored below.

Reactive Uptake Coefficients on Aqueous Solutions Covered with Organic Monolayers. The reactive uptake coefficients were determined from the irreversible removal of N₂O₅ as a function of injector position as mentioned above. Shown in Figure 3 are plots of the natural logarithm of the N₂O₅ signal as a function of reaction time for the loss of N₂O₅ on coated aqueous 60 wt % sulfuric acid solutions at 273 K. The data for each uptake experiment were fit to a straight line, and from the slope of this line, the first-order rate constant, k_{obs} , was determined. From k_{obs} , we calculated k_w and the reactive uptake coefficient.

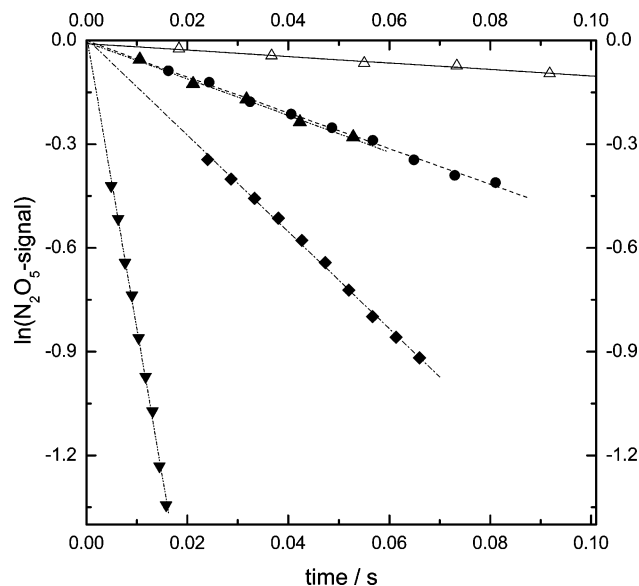


Figure 3. Natural logarithm of the observed N₂O₅ signal as a function of reaction time. Experiments were performed on aqueous 60 wt % H₂SO₄ solutions at 273 K. The lines represent the corresponding linear fits to the data. Open triangles, blank uptake; solid circles, 1-octadecanol; solid triangles, 1-hexadecanol; solid diamonds, stearic acid; solid inverted triangles, phytanic acid.

The reactive uptake coefficients for N₂O₅ on aqueous 60 wt % H₂SO₄ at 273 K in the presence of monolayers prepared with branched and straight-chain surfactants are reported in Table 2. The γ values reported in this study were based on at least six different uptake experiments performed on two or three freshly prepared monolayers. The upper and lower limits for γ take into account 20% error in the diffusion coefficients.

For organic coatings prepared with straight-chain surfactants, the reactive uptake coefficient was significantly less than that for the uncoated solutions. The reactive uptake coefficient for N₂O₅ on aqueous 60 wt % sulfuric acid coated with a monolayer of 1-octadecanol was $(8.0 \pm 1.7) \times 10^{-4}$, which is approximately a factor of 61 less than the observed uptake on aqueous 60 wt % H₂SO₄. Surfaces coated with monolayers of stearic acid and 1-hexadecanol showed a decrease in γ by factors of approximately 17 and 55, respectively, compared to the uncoated solution.

In Table 3 and Figure 4, we compare our results for the straight-chain surfactants with previous measurements reported

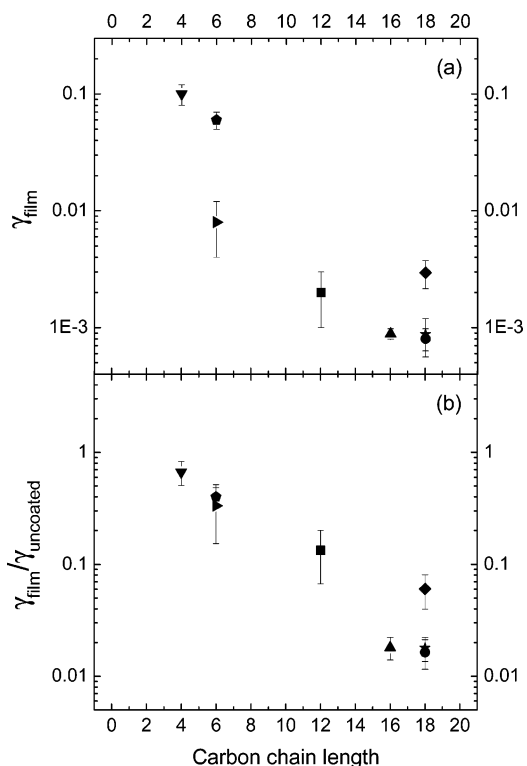


Figure 4. Reactive uptake coefficients of N₂O₅ on aqueous H₂SO₄ and NaCl solutions coated with straight-chain organic monolayers of different chain lengths: (a) γ_{film} , (b) $\gamma_{\text{film}}/\gamma_{\text{uncoated}}$. Solid circle, 1-octadecanol (this study); solid diamond, stearic acid (this study); solid triangle, 1-hexadecanol (this study); solid inverted triangle, 1-butanol (Park et al.);³¹ solid pentagon, hexanol (Park et al.);³¹ solid star, 1-octadecanol (Knopf et al.);³² solid sideways triangle, hexanoic acid (Thornton and Abbott);³⁰ solid square, SDS (McNeill et al.).²⁴

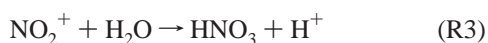
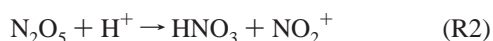
in the literature that also used straight-chain organic surfactants. Previous studies investigated monolayers of butanol, hexanol, hexanoic acid, sodium dodecyl sulfate (SDS), and 1-octadecanol.^{24,30–32} With the exception of 1-octadecanol, these molecules are all soluble species in the aqueous subphase and partition to the surface to form a surface excess. In Table 3, the reactive uptake coefficient in the presence of the organic film, γ_{film} , was normalized to the reactive uptake coefficient for the uncoated solutions, γ_{uncoated} , similarly to the approach of Park et al.³¹ In Figure 4, we plot both the reactive uptake coefficient, γ_{film} , and the normalized reactive uptake coefficient, $\gamma_{\text{film}}/\gamma_{\text{uncoated}}$. The data in both Table 3 and Figure 4 indicate that the reactive uptake coefficient decreases as the chain length increases.

For the reactive uptake of N_2O_5 in the presence of a branched monolayer of phytanic acid, we measured a γ value of $0.054^{+0.096}_{-0.015}$. This value is not statistically different from the reactive uptake coefficient corresponding to the uncoated 60 wt % $\text{H}_2\text{SO}_4\text{--H}_2\text{O}$ solution (see Table 2). Thus, the presence of the branched phytanic acid monolayer does not appear to significantly affect the reactive uptake of N_2O_5 .

Our work is the first to investigate the reactive uptake of N_2O_5 by aqueous H_2SO_4 solutions in the presence of branched monolayers. McNeill et al.³⁸ studied the loss of N_2O_5 on submicron aqueous NaCl particles coated with mixtures of oleate and oleic acid (bent aliphatic surfactant). They found that, when the aqueous particles were covered with a full monolayer, the N_2O_5 reactive uptake coefficient decreased by a factor of approximately 20. The difference between our results for a branched surfactant and the results by McNeill et al.³⁸ for a bent surfactant might be due to the structures of the monolayers or the difference in the aqueous subphases used in the two experiments. The latter point is discussed in more detail below.

The effect of branched surfactants or bent surfactants on the transfer rate of other gases across the air–aqueous interface has been studied in the past.^{26,28,62} Däumer et al.²⁶ showed that a coating of 1-(hydroxymethyl) adamantane (a branched hydrocarbon) had no significant effect on the neutralization rate of H_2SO_4 with NH_3 . Gilman and Vaida²⁸ demonstrated that the transport of acetic acid across the interface is impeded by long-chain organic molecules such as 1-octadecanol, but unaffected by bent molecules such as *cis*-9-octadecen-1-ol. Xiong et al.⁶² did not observe any retardation of the hygroscopic growth of acidic droplets by a single monolayer of oleic acid. However, care should be exercised when extrapolating these results to the N_2O_5 system, because a different mechanism might be important in each case and also each different study has a different sensitivity to a possible change in the reactive uptake coefficients or mass accommodation coefficients.

The mechanism responsible for the reaction between N_2O_5 and aqueous sulfuric acid solutions is believed to be an acid-catalyzed mechanism:^{63,64}



Also, the overall uptake of N_2O_5 by the H_2SO_4 aqueous solution can be expressed using the resistor model^{65–67}

$$\frac{1}{\gamma} = \frac{1}{S} + \frac{1}{\frac{1}{\Gamma_{\text{b}}} + \frac{1}{S \frac{k_{\text{sol}}}{k_{\text{desorb}}}}} + \Gamma_{\text{surf}} \quad (4)$$

where S is the sticking coefficient (fraction of collisions at the surface that result in accommodation on the surface); k_{sol} is the rate coefficient for the transfer from the surface into the liquid; k_{desorb} is the rate coefficient for the transfer of molecules from the surface into the gas phase; Γ_{b} is the rate of reaction in the bulk of the solution, normalized to the gas-phase collision frequency; and Γ_{surf} represents the surface reaction.

The presence of the organic monolayer can influence γ in a number of different ways. First, the monolayer can influence the sticking coefficient, S , of N_2O_5 on the surface and/or the transfer of N_2O_5 molecules from the surface into the liquid (k_{sol}), by acting as a barrier to mass transfer. In addition, the organic monolayer could influence possible surface reactions by modifying Γ_{surf} . We assume that the presence of the monolayer does not influence the bulk reaction rate. Also, if the hydrolysis reaction occurs close to the surface, the carboxylic and/or alcohol functional groups on the surfactant molecules could potentially play a role. However, from our results, the reactive uptake coefficient correlates best with the packing density of the organic surfactants, not the functional groups on the surfactants (see below for more details).

Correlations between Reactive Uptake Coefficients and Carbon Chain Length, Surface Pressure, and Molecular Surface Area. The reactive uptake coefficient is expected to be a function of several parameters including the molecular surface area of the surfactant, the carbon chain length, the structure of the surfactant, the surface pressure, and the aqueous subphase. In the following analysis, we compare measured γ values with several of these parameters (carbon chain length, surface pressure, and molecular surface area) to determine whether one of these parameters dominates the reactive uptake coefficient. For the first part of this analysis, we used only our data and the data from Park et al.³¹ and Knopf et al.³² because these data sets were all obtained with the same subphase (aqueous sulfuric acid solutions). The experiments of Park et al.³¹ were carried out on 72 wt % H_2SO_4 solution at 216 K. We assume here that our data, obtained at 273 K, are directly comparable to the data obtained by Park et al.;³¹ however, further work is needed to verify this assumption. After this analysis, we also discuss the results obtained with other subphases.

In Figure 5, the reactive uptake coefficient measured on aqueous sulfuric acid solutions is plotted as a function. Figure 5a shows γ_{film} , and Figure 5b shows $\gamma_{\text{film}}/\gamma_{\text{uncoated}}$, similar to Park et al.³¹ The solid symbols are results for straight-chain organic surfactants including data obtained in this study and those reported in the literature.^{31,32} The open symbols represent the results obtained in this study for the branched monolayer. For the straight-chain surfactants, there appears to be a correlation between γ and the length of the hydrocarbon chain, although there is some scatter in the data for carbon chain lengths between C16 and C18. This scatter might be due to differences in the properties used in the different experiments, such as molecular surface area (see below). Nevertheless, a trend is apparent. In contrast, the branched result deviates dramatically from the straight-chain trend.

The reactive uptake coefficient is plotted as a function of surface pressure in Figure 6. Figure 6a shows γ_{film} , and Figure 6b shows $\gamma_{\text{film}}/\gamma_{\text{uncoated}}$. As in Figure 5, the solid symbols correspond to the results for straight-chain surfactants, and the open symbols correspond to the branched surfactant. Clearly, γ_{film} and $\gamma_{\text{film}}/\gamma_{\text{uncoated}}$ do not correlate with the surface pressure of the films.

In Figure 7, the reactive uptake coefficient is plotted as a function of the surface area occupied by each surfactant

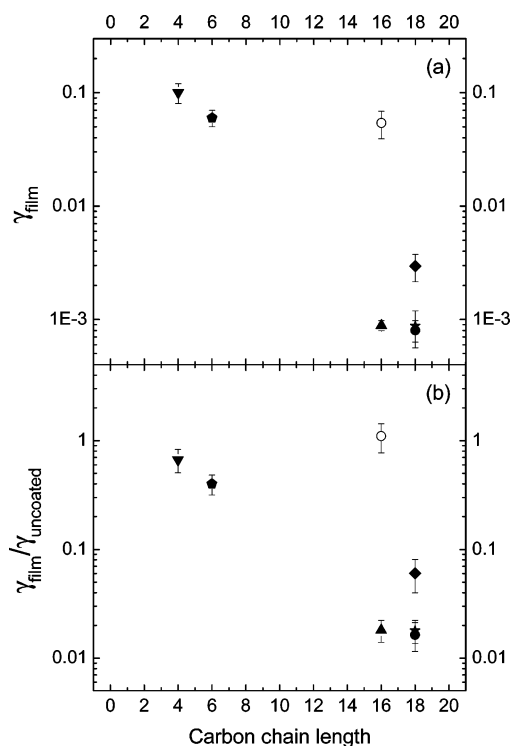


Figure 5. Reactive uptake coefficients for N₂O₅ on organic-coated sulfuric acid solutions as a function of carbon chain length: (a) γ_{film} , (b) $\gamma_{\text{film}}/\gamma_{\text{uncoated}}$. Solid symbols represent straight-chain molecules, and open symbols represent the branched molecule. Solid circle, 1-octadecanol (this study); solid diamond, stearic acid (this study); solid triangle, 1-hexadecanol (this study); open circle, phytanic acid (this study); solid inverted triangle, 1-butanol (Park et al.);³¹ solid pentagon, hexanol (Park et al.);³¹ solid star, 1-octadecanol (Knopf et al.).³²

molecule. The solid symbols correspond to the results for straight-chain surfactants, and the open symbols correspond to the results for the branched surfactant. The dashed line represents a sigmoidal fit (Figure 7) to the straight-chain data. This fit was chosen because it resulted in the best fit to the data. However, it serves solely to guide the eye. The data corresponding to the surfactants follow a trend: as the molecular surface area decreases, the reactive uptake coefficient decreases. This is to be expected, because, as the molecular surface area decreases, the monolayer becomes more densely packed and should limit the transfer of N₂O₅ across the air–aqueous interface. Within the experimental uncertainty, the reactive uptake coefficient obtained for the branched surfactant follows the trend observed for the reactive uptake coefficients obtained for the straight-chain surfactants. Therefore, we speculate that the reason that the γ values of the branched monolayers do not decrease significantly is because these monolayers are not densely packed. On the basis of this very limited set of data, we suggest that the molecular surface area is the best parameter for predicting the influence of an organic monolayer on the reactive uptake coefficient (at least for an aqueous sulfuric acid subphase) because it can explain, reasonably well, the trends for both the straight-chain surfactants and the branched surfactants.

In Figures 5–7, we include only data obtained with an aqueous sulfuric acid subphase. In Figure 8, we also include data corresponding to aqueous sea salt aerosols and aqueous NaCl particles. The solid symbols correspond to data obtained with an aqueous sulfuric acid subphase (the same data as were shown in Figure 7), and the open symbols correspond to data obtained with other subphases. Thornton and Abbatt³⁰ studied

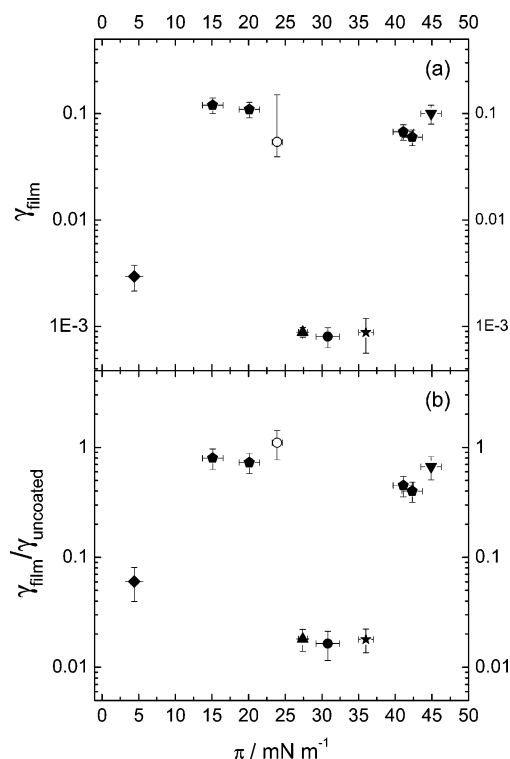


Figure 6. Reactive uptake coefficients for N₂O₅ on organic-coated aqueous sulfuric acid solutions as a function of monolayer surface pressure: (a) γ_{film} , (b) $\gamma_{\text{film}}/\gamma_{\text{uncoated}}$. Solid symbols represent straight-chain molecules, and open symbols represent the branched molecule. Solid circle, 1-octadecanol (this study); solid diamond, stearic acid (this study); solid triangle, 1-hexadecanol (this study); open circle, phytanic acid (this study); solid inverted triangle, butanol (Park et al.);³¹ solid pentagon, hexanol (Park et al.);³¹ solid star, 1-octadecanol (Knopf et al.).³²

the loss of N₂O₅ on aqueous sea salt aerosols coated with hexanoic acid (straight-chain C6 surfactant). McNeill et al.²⁴ studied the reactive uptake coefficient on aqueous NaCl aerosols coated with sodium dodecyl sulfate (straight-chain C12 surfactant), and McNeill et al.³⁸ studied the loss of N₂O₅ on submicron aqueous NaCl particles coated with mixtures of oleate and oleic acid (bent C18 surfactant). In the studies by Thornton and Abbatt,³⁰ the molecular surface areas were estimated from bulk surface tension measurements. Both studies by McNeill et al.^{24,38} estimated the molecular surface areas of their monolayers indirectly from an observed plateau in the kinetics N₂O₅ uptake data.

It is apparent that the data obtained with an aqueous sulfuric acid subphase are not in agreement with those obtained using other subphases when the reactive uptake coefficient is plotted versus the molecular surface area. The reason for the difference is not clear, but perhaps it suggests that different mechanisms are important for the different subphases. Alternatively, molecular surface area might be only one of the important parameters, and other variables need to be considered when assessing the overall reactivity and explaining all of the experimental data. Yet another alternative might be related to the experimental techniques. All of the aqueous sulfuric acid experiments were carried out with bulk solutions coated with surfactants, whereas the other experiments were all carried out with aerosols. As pointed out by McNeill et al.^{24,38} and Thornton and Abbatt,³⁰ their aerosol generation method leads to uncertainty in the actual mixing state of the surface-active organics. Nonetheless, their interpretation of the N₂O₅ kinetics yields predictions of areas per molecule that are strikingly similar to

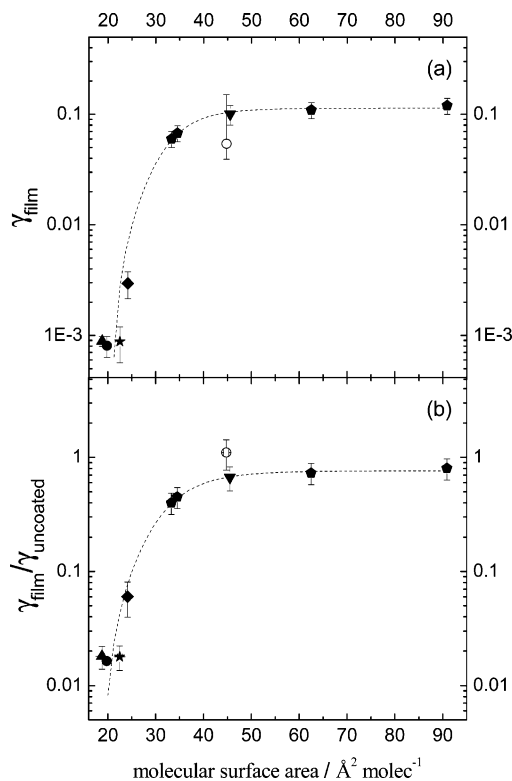


Figure 7. Reactive uptake coefficients for N_2O_5 on organic-coated aqueous sulfuric acid solutions as a function of packing density: (a) γ_{film} , (b) $\gamma_{\text{film}}/\gamma_{\text{uncoated}}$. Solid symbols represent straight-chain molecules, and open symbols represent the branched molecule. Solid circle, 1-octadecanol (this study); solid diamond, stearic acid (this study); solid triangle, 1-hexadecanol (this study); open circle, phytanic acid (this study); solid inverted triangle, butanol (Park et al.);³¹ solid pentagon, hexanol (Park et al.);³¹ solid star, 1-octadecanol (Knopf et al.).³² The dashed line represents a sigmoidal fit to the straight-chain molecules. This fit was chosen because it gave a reasonable fit to the data, but it has no physical meaning.

equilibrium values determined on macroscopic systems. Although perhaps the aerosol measurements with NaCl or seawater aerosols are not directly comparable to the sulfuric acid data, the differences illustrated in Figure 8 suggest that the nature of the subphase might play an important role in the effect of surface-active organics on the net reactive uptake. Also interesting, in contrast to Figure 8, is the fact that the data from McNeill et al.^{24,38} and Thornton and Abbatt³⁰ are in good agreement with the data obtained with aqueous sulfuric acid subphases (except for our phytanic acid data) when the reactive uptake coefficient is plotted against the carbon chain length (see Table 3 and Figure 4). The issues mentioned above should be addressed by future experiments.

4. Atmospheric Implications

Our results suggest that insoluble straight-chain organic surfactants can decrease the reactive uptake coefficient by a factor of 17–61. This decrease in the reactive uptake coefficient is of the same order of magnitude as the decrease in reactive uptake coefficient observed by Brown et al.³⁷ during a recent field measurement over the northeast United States. They showed that the reactive uptake coefficient of N_2O_5 can decrease significantly (by a factor of ≥ 10) when particles contain a large amount of organic material in addition to inorganic material. However, keep in mind that, when Brown et al.³⁷ observed a dramatic decrease in the reactive uptake coefficient, the inorganic material consisted of ammonium sulfate. Conse-

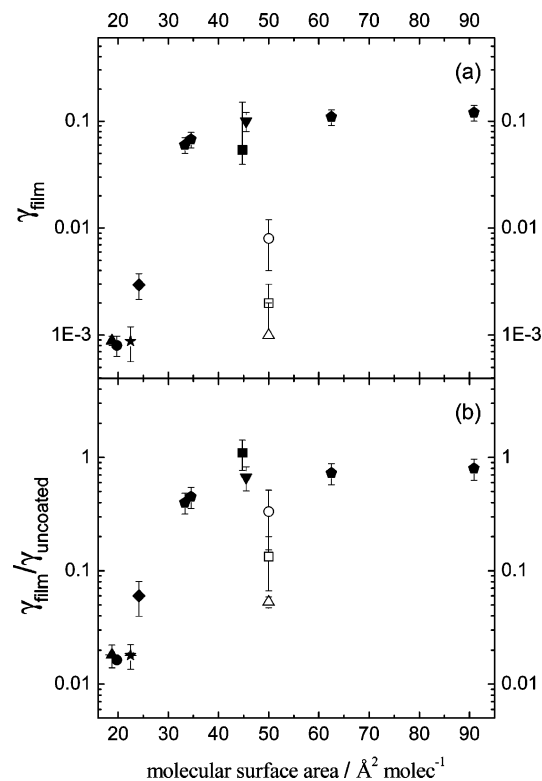


Figure 8. Reactive uptake coefficients for N_2O_5 on aqueous solutions and aerosols as a function of packing density: (a) γ_{film} , (b) $\gamma_{\text{film}}/\gamma_{\text{uncoated}}$. Solid symbols represent data collected on aqueous sulfuric acid subphases, and open symbols represent data collected on other subphases. Solid circle, 1-octadecanol (this study); solid diamond, stearic acid (this study); solid triangle, 1-hexadecanol (this study); solid square, phytanic acid (this study); solid inverted triangle, butanol (Park et al.);³¹ solid pentagon, hexanol (Park et al.);³¹ solid star, 1-octadecanol (Knopf et al.);³² open circle, hexanoic acid (Thornton and Abbatt);³⁰ open square, SDS (McNeill et al.);²⁴ open triangle, oleate (McNeill et al.).³⁸

quently, our results might not be directly comparable to the field measurements by Brown et al.³⁷ because we used a different subphase. Experiments with an aqueous ammonium sulfate subphase would be beneficial.

In contrast to straight-chain monolayers, phytanic acid (an insoluble branched monolayer) showed no significant effect on the uptake of N_2O_5 (the decrease in the uptake coefficient was less than the uncertainty in our measurements). This result highlights the need for studies that focus on the physical and chemical properties of organic surfactants that reside on the surface of aqueous particles in the atmosphere. Researchers have begun to consider the detailed structure of organic monolayers on aerosol particles (see for example Seidl⁶⁸), but more studies in this direction would be beneficial. Also, studies that investigate the effects of other types of branched and bent surfactants on the reactive uptake of N_2O_5 employing atmospherically relevant subphases would be helpful. In the atmosphere, aerosol particles most likely consist of a mixture of different organic surfactants. Studies on the effects of mixed monolayers (i.e., monolayers containing both straight-chain and branched surfactants) would also be informative.

5. Summary and Conclusions

A rectangular channel flow reactor coupled to a chemical ionization mass spectrometer was used to study the reactive uptake coefficients of N_2O_5 on aqueous 60 wt % sulfuric acid solutions at 273 K coated with insoluble organic monolayers.

Both straight-chain (1-hexadecanol, 1-octadecanol, and stearic acid) and branched (phytanic acid) monolayers were studied. The reactive uptake coefficients obtained were $(8.9 \pm 0.9) \times 10^{-4}$, $(8.0 \pm 1.7) \times 10^{-4}$, $(3.0 \pm 0.8) \times 10^{-3}$, and $(5.4_{-1.5}^{+9.6}) \times 10^{-2}$ for 1-hexadecanol, 1-octadecanol, stearic acid, and phytanic acid, respectively. The reactive uptake coefficient decreased dramatically for straight-chain surfactants. The decrease ranged from a factor of 17 to a factor of 61 depending on the type of straight-chain surfactant. In contrast to the straight-chain data, N₂O₅ uptake in the presence of phytanic acid, which has a branched structure, did not have a significant effect on the N₂O₅ reactive uptake coefficient (the decrease was less than the uncertainty in the data) compared to the uncoated solution.

In addition to measuring the reactive uptake coefficients, we also tried to correlate properties of the monolayers with the reactive uptake coefficients. Judging from a limited set of data, the reactive uptake coefficients measured on aqueous sulfuric acid subphases coated with organic monolayers show a relationship to the molecular surface area occupied by each surfactant molecule. The apparent correlation between γ and the molecular surface area of the surfactant can be tentatively explained by the fact that mass transport is hindered by tight-packed surfactants compared to less densely packed ones (branched surfactants). This leads to the possible conclusion that the overall uptake process is governed by mass transport rather than by reaction. On the other hand, the aqueous subphase seems to influence γ significantly (see Figure 8), which suggests a dependence on the reaction mechanism. This apparent complexity should be investigated with future studies. Our results also highlight the need for further studies that focus on the physical and chemical properties of the organic surfactants that reside on the surface of aqueous particles in the atmosphere.

Acknowledgment. This work was funded by the Natural Science and Engineering Research Council of Canada (NSERC), the Canadian Foundation for Climate and Atmospheric Sciences (CFCAS), and the Canada Foundation for Innovation (CFI). J. Mak and S. Gross are acknowledged for help during the development of the N₂O₅ source. We also thank D. Bizzotto for helpful discussions on monolayer preparation and characterization. We also thank J. A. Thornton, V. F. McNeill, and S. S. Brown for several helpful discussions related to the manuscript.

References and Notes

- (1) Poschl, U. *Angew. Chem., Int. Ed.* **2005**, *44*, 7520–7540.
- (2) Zhang, Y.; Carmichael, G. R. *J. Appl. Meteorol.* **1999**, *38*, 353–366.
- (3) Molina, M. J.; Molina, L. T.; Kolb, C. E. *Annu. Rev. Phys. Chem.* **1996**, *47*, 327–367.
- (4) Ravishankara, A. R. *Science* **1997**, *276*, 1058–1065.
- (5) Dentener, F. J.; Crutzen, P. J. *J. Geophys. Res. D: Atmos.* **1993**, *98*, 7149–7163.
- (6) Evans, M. J.; Jacob, D. J. *Geophys. Res. Lett.* **2005**, *32*, L09813, doi:09810.01029/02005GL022469.
- (7) Tie, X.; Brasseur, G.; Emmons, L.; Horowitz, L.; Kinnison, D. J. *Geophys. Res. D: Atmos.* **2001**, *106*, 22931–22964.
- (8) Sander, S. P.; Golden, D. M.; Kurylo, M. J.; Moortgat, G. K.; Wine, P. H.; Ravishankara, A. R.; Kolb, C. E.; Molina, M. J.; Finlayson-Pitts, B. J.; Huie, R. E. *Chemical Kinetics and Photochemical Data for Use in Atmospheric Studies Evaluation Number 15*; JPL Publication 06-2; Jet Propulsion Laboratory: Pasadena, CA, 2006.
- (9) Barger, W. R.; Garrett, W. D. *J. Geophys. Res.* **1970**, *75*, 4561–4566.
- (10) Barger, W. R.; Garrett, W. D. *J. Geophys. Res. C: Oceans Atmos.* **1976**, *81*, 3151–3157.
- (11) Cavalli, F.; Facchini, M. C.; Decesari, S.; Mircea, M.; Emblico, L.; Fuzzi, S.; Ceburnis, D.; Yoon, Y. J.; O'Dowd, C. D.; Putaud, J. P.; Dell'Acqua, A. *J. Geophys. Res. D: Atmos.* **2004**, *109*, D24215, doi:24210.21029/22004JD0051137.
- (12) Decesari, S.; Facchini, M. C.; Fuzzi, S.; Tagliavini, E. *J. Geophys. Res. D: Atmos.* **2000**, *105*, 1481–1489.
- (13) Mochida, M.; Kitamori, Y.; Kawamura, K.; Nojiri, Y.; Suzuki, K. *J. Geophys. Res.* **2002**, *107*, 4325, doi:4310.1029/2001JD001278.
- (14) O'Dowd, C. D.; Facchini, M. C.; Cavalli, F.; Ceburnis, D.; Mircea, M.; Decesari, S.; Fuzzi, S.; Yoon, Y. J.; Putaud, J. P. *Nature* **2004**, *431*, 676–680.
- (15) Peterson, R. E.; Tyler, B. J. *Appl. Surf. Sci.* **2003**, *203*, 751–756.
- (16) Peterson, R. E.; Tyler, B. J. *Atmos. Environ.* **2002**, *36*, 6041–6049.
- (17) Russell, L. M.; Maria, S. F.; Myneni, S. C. B. *Geophys. Res. Lett.* **2002**, *29*, 1779, doi:10.1029/2202GL014874.
- (18) Tervahattu, H.; Hartonen, K.; Kerminen, V. M.; Kupiainen, K.; Aarnio, P.; Koskentalo, T.; Tuck, A. F.; Vaida, V. *J. Geophys. Res. D: Atmos.* **2002**, *107*, 4053, doi:4010.1029/2000JD000282.
- (19) Tervahattu, H.; Juhanaja, J.; Kupiainen, K. *J. Geophys. Res. D: Atmos.* **2002**, *107*, 4319, doi:4310.1029/2001JD001403.
- (20) Tervahattu, H.; Juhanaja, J.; Vaida, V.; Tuck, A. F.; Niemi, J. V.; Kupiainen, K.; Kulmala, M.; Vehkamäki, H. *J. Geophys. Res. D: Atmos.* **2005**, *110*, D06207, doi:06210.01029/02004JD005400.
- (21) Ellison, G. B.; Tuck, A. F.; Vaida, V. *J. Geophys. Res. D: Atmos.* **1999**, *104*, 11633–11641.
- (22) Gill, P. S.; Graedel, T. E.; Weschler, C. J. *Rev. Geophys.* **1983**, *21*, 903–920.
- (23) Donaldson, D. J.; Vaida, V. *Chem. Rev.* **2006**, *106*, 1445–1461.
- (24) McNeill, V. F.; Patterson, J.; Wolfe, G. M.; Thornton, J. A. *Atmos. Chem. Phys.* **2006**, *6*, 1635–1644.
- (25) Anttila, T.; Kiendler-Scharr, A.; Tillmann, R.; Mentel, T. F. *J. Phys. Chem. A* **2006**, *110*, 10435–10443.
- (26) Daumer, B.; Niessner, R.; Klockow, D. *J. Aerosol Sci.* **1992**, *23*, 315–325.
- (27) Folkers, M.; Mentel, T. F.; Wahner, A. *Geophys. Res. Lett.* **2003**, *30*, 1644, doi:1610.1029/2003GL017168.
- (28) Gilman, J. B.; Vaida, V. *J. Phys. Chem. A* **2006**, *110*, 7581–7587.
- (29) Lawrence, J. R.; Glass, S. V.; Park, S. C.; Nathanson, G. M. *J. Phys. Chem. A* **2005**, *109*, 7458–7465.
- (30) Thornton, J. A.; Abbatt, J. P. D. *J. Phys. Chem. A* **2005**, *109*, 10004–10012.
- (31) Park, S. C.; Burden, D. K.; Nathanson, G. M. *J. Phys. Chem. A* **2007**, *111*, 2921–2929.
- (32) Knopf, D. A.; Cosman, L. M.; Mousavi, P.; Mokamati, S.; Bertram, A. K. *J. Phys. Chem. A* **2007**, *111*, 11021–11032.
- (33) Clifford, D.; Bartels-Rausch, T.; Donaldson, D. J. *Phys. Chem. Chem. Phys.* **2007**, *9*, 1362–1369.
- (34) Barnes, G. T. *Colloids Surf. A* **1997**, *126*, 149–158.
- (35) Jefferson, A.; Eisele, F. L.; Ziemann, P. J.; Weber, R. J.; Marti, J. J.; McMurry, P. H. *J. Geophys. Res. D: Atmos.* **1997**, *102*, 19021–19028.
- (36) Rubel, G. O.; Gentry, J. W. *J. Aerosol Sci.* **1985**, *16*, 571–574.
- (37) Brown, S. S.; Ryerson, T. B.; Wollny, A. G.; Brock, C. A.; Peltier, R.; Sullivan, A. P.; Weber, R. J.; Dube, W. P.; Trainer, M.; Meagher, J. F.; Fehsenfeld, F. C.; Ravishankara, A. R. *Science* **2006**, *311*, 67–70.
- (38) McNeill, V. F.; Wolfe, G. M.; Thornton, J. A. *J. Phys. Chem. A* **2007**, *111*, 1073–1083.
- (39) Kanakidou, M.; Seinfeld, J. H.; Pandis, S. N.; Barnes, I.; Dentener, F. J.; Facchini, M. C.; Van Dingenen, R.; Ervens, B.; Nenes, A.; Nielsen, C. J.; Swietlicki, E.; Putaud, J. P.; Balkanski, Y.; Fuzzi, S.; Horth, J.; Moortgat, G. K.; Winterhalter, R.; Myhre, C. E. L.; Tsigaridis, K.; Vignati, E.; Stephanou, E. G.; Wilson, J. *Atmos. Chem. Phys.* **2005**, *5*, 1053–1123.
- (40) Badger, C. L.; Griffiths, P. T.; George, I.; Abbatt, J. P. D.; Cox, R. A. *J. Phys. Chem. A* **2006**, *110*, 6986–6994.
- (41) Massucci, M.; Clegg, S. L.; Brimblecombe, P. J. *Phys. Chem. A* **1999**, *103*, 4209–4226.
- (42) Wexler, A. S.; Clegg, S. L. *J. Geophys. Res.* **2002**, *107*, 4207, doi:4210.1029/2001JD000451.
- (43) Carslaw, K. S.; Clegg, S. L.; Brimblecombe, P. J. *Phys. Chem.* **1995**, *99*, 11557–11574.
- (44) Knopf, D. A.; Anthony, L. M.; Bertram, A. K. *J. Phys. Chem. A* **2005**, *109*, 5579–5589.
- (45) Knopf, D. A.; Mak, J.; Gross, S.; Bertram, A. K. *Geophys. Res. Lett.* **2006**, *33*, L17816, doi:17810.11029/12006GL026884.
- (46) Huey, L. G.; Hanson, D. R.; Howard, C. J. *J. Phys. Chem.* **1995**, *99*, 5001–5008.
- (47) Hu, J. H.; Abbatt, J. P. D. *J. Phys. Chem. A* **1997**, *101*, 871–878.
- (48) Thornton, J. A.; Braban, C. F.; Abbatt, J. P. D. *Phys. Chem. Chem. Phys.* **2003**, *5*, 4593–4603.
- (49) Mason, E. A.; Monchick, L. *J. Chem. Phys.* **1962**, *36*, 2746–2757.
- (50) Monchick, L.; Mason, E. A. *J. Chem. Phys.* **1961**, *35*, 1676–1697.
- (51) Patrick, R.; Golden, D. M. *Int. J. Chem. Kinet.* **1983**, *15*, 1189–1227.
- (52) Hanson, D. R.; Ravishankara, A. R. *J. Geophys. Res.* **1991**, *96*, 5081–5090.
- (53) Hanson, D. R. *J. Phys. Chem. A* **1998**, *102*, 4794–4807.
- (54) Motz, H.; Wise, H. *J. Chem. Phys.* **1960**, *32*, 1893–1894.

- (55) Gaines, G. L., Jr. *Insoluble Monolayers at Liquid–Gas Interfaces*; Interscience Publishers: New York, 1966.
- (56) Rolo, L. I.; Caco, A. I.; Queimada, A. J.; Marrucho, I. M.; Coutinho, J. A. P. *J. Chem. Eng. Data* **2002**, *47*, 1442–1445.
- (57) Adamson, A. W.; Gast, A. P. *Physical Chemistry of Surfaces*, 6th ed.; Wiley-Interscience: New York, 1997.
- (58) Myrick, S. H.; Franses, E. I. *Colloids Surf. A* **1998**, *143*, 503–515.
- (59) Vines, R. G. *Q. J. R. Meteorol. Soc.* **1959**, *85*, 159–162.
- (60) Lawrie, G. A.; Barnes, G. T. *J. Colloid Interface Sci.* **1994**, *162*, 36–44.
- (61) Kaganer, V. M.; Mohwald, H.; Dutta, P. *Rev. Mod. Phys.* **1999**, *71*, 779–819.
- (62) Xiong, J. Q.; Zhong, M. H.; Fang, C. P.; Chen, L. C.; Lippmann, M. *Environ. Sci. Technol.* **1998**, *32*, 3536–3541.
- (63) Hallquist, M.; Stewart, D. J.; Baker, J.; Cox, R. A. *J. Phys. Chem. A* **2000**, *104*, 3984–3990.
- (64) Robinson, G. N.; Worsnop, D. R.; Jayne, J. T.; Kolb, C. E.; Davidovits, P. *J. Geophys. Res. D: Atmos.* **1997**, *102*, 3583–3601.
- (65) Schwartz, S. E. *Chemistry of Multiphase Atmospheric Systems*; NATO ASI Series; Springer-Verlag: Berlin, 1986.
- (66) Jayne, J. T.; Duan, S. X.; Davidovits, P.; Worsnop, D. R.; Zahniser, M. S.; Kolb, C. E. *J. Phys. Chem.* **1992**, *96*, 5452–5460.
- (67) Hanson, D. R. *J. Phys. Chem. B* **1997**, *101*, 4998–5001.
- (68) Seidl, W. *Atmos. Environ.* **2000**, *34*, 4917–4932.